Journal of Ceramic Processing Research. Vol. 18, No. 1, pp. 16~20 (2017)

J O U R N A L O F
Ceramic Processing Research

Simultaneous synthesis and consolidation of nanocrystalline 4Al-3SiC composite by high-frequency induction heating

In-Jin Shon[a,*] and Woo-Jeong Kim[b]
[a]*Division of Advanced Materials Engineering, Research Center of Advanced Materials Development, Chonbuk National University, 664-14 Deokjin-dong 1-ga, Deokjin-gu, Jeonju, Jeonbuk 561-756, Korea*
[b]*Wonjin Aluminium, 416 Technovalley-ro, Bongdong-eup, Wanju-gun, Jeollabuk-do, Korea*

Nanopowders of Si and Al_4C_3 were made by high energy ball milling. The average grain sizes of Al_4C_3 and Si measured by Suryanarayana and Grant Norton's formula were about 33 and 18 nm, respectively. Highly dense nanostructured 4Al-3SiC composite was consolidated by high-frequency induction heated sintering method within two minutes from the mechanically activated powders under the 80 MPa pressure. The microstructure and mechanical properties (hardness and fracture toughness) were investigated using FE-SEM and Vickers hardness tester.

Key words: Rapid sintering, Composite, Nanomaterial, Mechanical properties, Co-ZrO_2.

Introduction

The continuous increase in the performance requirement of materials for aerospace and automotive applications have lead to development of several structural composite materials. Among these, metal matrix composites refer to a kind of material in which rigid ceramic reinforcements are embedded in a ductile metal or alloy matrix. Metal matrix composites combine metallic properties (ductility and toughness) with ceramic characteristics (high strength and modulus), leading to greater strength in shear and compression and to higher service temperature capabilities. The attractive physical and mechanical properties that can be obtained with metal matrix composites, such as high specific modulus, strength-to weigh ratio, fatigue strength, and temperature stability and wear resistance, have been documented extensively [1].

SiC has a low density, high hardness, chemical stability, low thermal expansion, and high strength at high temperatures. In addition, SiC is a wide gap semiconductor with a high electric breakdown threshold, and thus is attractive as an electronic material for special applications [2]. Al has a low density and good fracture toughness. Hence, microstructure consisting of Al and SiC may be able to satisfy the good mechanical properties requirements of successful structural material.

Nanocrystalline materials, as advanced engineering materials, have received much attention due to their improved physical and mechanical properties [3, 4]. Recently, nanocrystalline powders have been produced by high-energy milling [5, 6]. The sintering temperature of high-energy mechanically milled powder is lower than that of unmilled powder due to the increased reactivity, internal and surface energies, and surface area of the milled powder, which contribute to its so-called mechanical activation [7-9]. The grain size in sintered materials, however, becomes much larger than that in pre-sintered powders due to a rapid grain growth during conventional sintering process. Therefore, controlling grain growth during sintering is one of the keys to the commercial success of nanostructured materials. In this regard, the high-frequency induction heated sintering method which can make dense materials within 3 min, has been shown to be effective in achieving this goal [10-12].

The purpose of this work is to produce nanopowders of Si, Al_4C_3 and synthesis and consolidation of nanocrystalline 4Al-3SiC composite within 2 minutes from mechanically activated powders (3Si-Al_4C_3) using this high-frequency induction heated sintering method. Microstructure and mechanical properties (hardness and fracture toughness) of the composite were also evaluated.

Experimental Procedure

The Al_4C_3 powder with a purity of 99% (< 45 μm, Alfa Aesar, Inc.) and Si powder with a purity of 99.9985% (< 20 μm, Alfa Aesar, Inc.) were used as raw materials. The Al_4C_3 and Si powders with ratio of 1 : 3 were mixed using a high-energy ball mill (i.e., a Pulverisette-5 planetary mill) at 200 rpm for 10 hrs under a 99.9999% pure Ar atmosphere. Tungsten carbide balls with a diameter of 10 mm were used in a

*Corresponding author:
Tel : +82-63-270-2381
Fax: +82-63-270-2386
E-mail: ijshon@chonbuk.ac.kr

sealed cylindrical stainless steel vial. The weight ratio of ball-to-powder was 20 : 1.

The milled powder was put in a graphite die which was sealed between upper and lower graphite punches. The graphite die was cylindrical, with a 35 mm outside diameter and a 10 mm inside diameter with a height of 40 mm. The high-frequency induction heated sintering system made by Eltek in South Korea is shown schematically in many references [10-12]. The sintering process has the four distinguishable stages as follows. Stage 1: the evacuating the system. Stage 2: applying a mechanically uniaxial pressure of 80 MPa. Stage 3: activating an induced current. The temperature was reached at 1500 °C with a heating rate of 1400 °C/min. and then the current was turned off immediately. A pyrometer focused on the surface of the graphite die was used to measure the temperature. Stage 4: cooling the sintered sample to room temperature. All process was carried out under a vacuum of 10 Pa.

The Archimedes principle was adopted to measure the relative density of the sintered sample. Microstructure was observed from the sintered sample after polishing and etching. Compositional and microstructural features of the products were analyzed using X-ray diffraction (XRD), scanning electron microscopy (SEM) with energy dispersive spectroscopy (EDS) and field emission scanning electron microscopy (FE-SEM). Vickers hardness was measured by performing indentations at a load of 196 N and a dwell time of 15 s. The average grain sizes of SiC and Al was calculated using the formula proposed by Suryanarayana and Grant Norton [13].

Results and Discussion

The interaction between Al_4C_3 and 3 Si, i.e.;

$$Al_4C_3 + 3\ Si \rightarrow 4\ Al + 3\ SiC \quad (1)$$

is thermodynamically feasible as shown in Fig. 1.

Fig. 2 shows the X-ray diffraction patterns of raw powder of (a) Al_4C_3, (b) Si and (c) mechanically high energy ball milled powders from raw powders. In Fig. 2(c), products (Al and SiC) were not detected and reactants of Al_4C_3 and Si were observed. From above results, solid replacement reaction completely did not occur during the high energy ball milling. The full width at half-maximum (FWHM) of the diffraction peak in Fig. 2(c) is broad due to refinement of powder and strain. Plots of Br cosθ versus sinθ for (a) Al_4C_3 and (b) Si powders milled by high energy ball milling for 10 hrs show in Fig. 3. The average grain sizes of Al_4C_3 and Si measured by Suryanarayana and Grant Norton's formula were about 33 and 18 nm, respectively. Fig. 4 shows FE-SEM image and EDS analysis of milled powders. The powders are very fine and have some agglomeration. In EDS, the peaks of Si, C and Al were analyzed, and there are no other peaks, such as Fe or

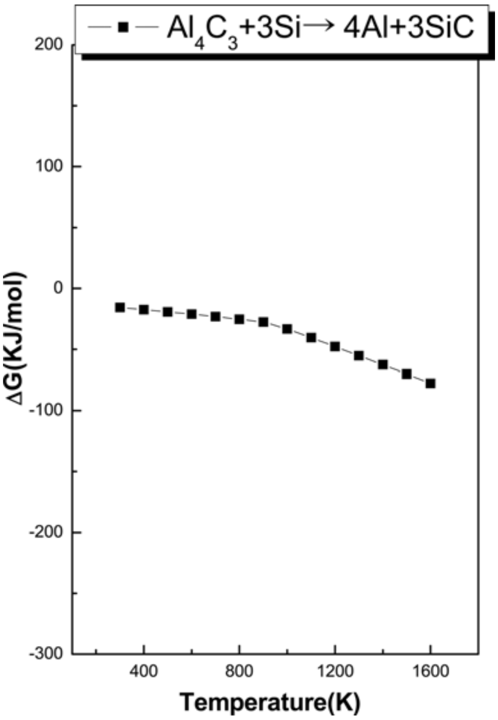

Fig. 1. Temperature dependence of the Gibbs free energy variation by interaction of Al_4C_3 with 3Si.

W, which can possibly happen during the milling process.

The variation of shrinkage displacement and temperature with heating time, during densification of milled powders, is shown in Fig. 5. The application of the induced current resulted in shrinkage, due to consolidation and synthesis. The abrupt increase in the shrinkage displacement is due to the increase in density as a result of molar volume change associated with the formation of 3SiC and 4Al from 3Si and Al_4C_3 reactant and the consolidation of the product. As the induced current was applied, thermal expansion was shown up to 900 °C, and then shrinkage displacement gradually increased above that temperature. XRD pattern of the high-energy ball milled powder heated to 1500? is shown in Fig. 6. Al and SiC peaks are mainly detected. From X-ray pattern of Fig. 6, 4Al-3SiC was synthesized from milled powders of $Al_4C_3 + 3$ Si. Fig. 7 shows plot of $B_r \cos\theta$ versus sinθ to calculate grain size of Al and SiC. The structure parameters, i.e. the average grain sizes of Al and SiC in composite sintered from high energy ball milled powder obtained from X-ray data in Fig. 7 by Suryanarayana and Grant Norton's formula, are 37, 39 nm, respectively. Fig. 8 shows FE-SEM image and EDS analysis of 4Al-3SiC composite sintered at 1500 °C from high energy ball milled powders. The composites consist of nanograins. Dark area and grey area in FE-SEM are SiC and Al from EDS analysis and mass contrast, respectively. And the relative density of the 4Al-3SiC composite was 97%. It is considered that the reasons of high density and nanostructure of the

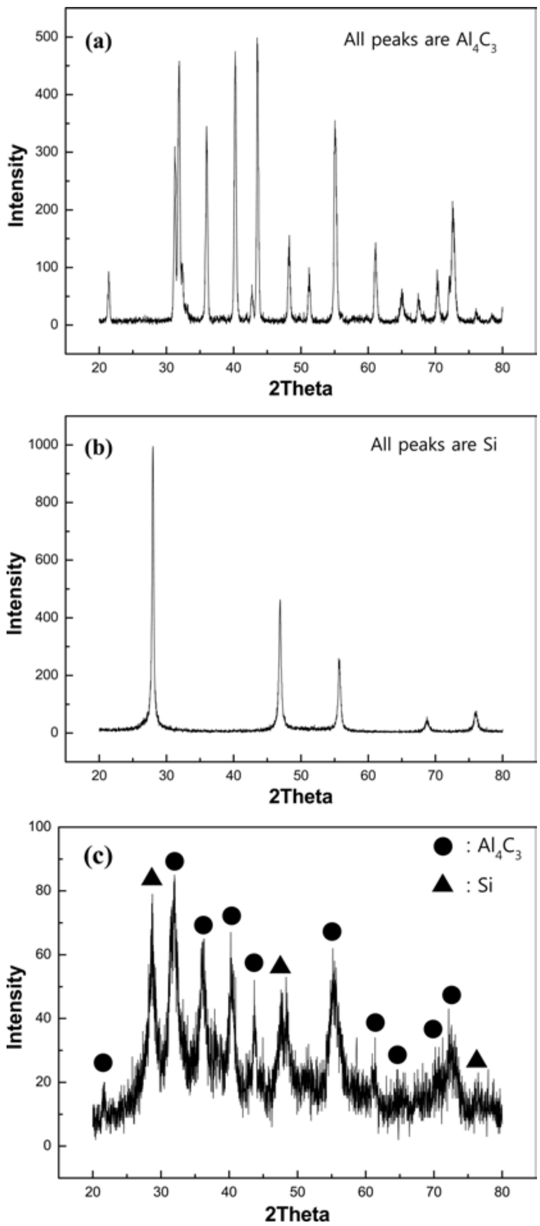

Fig. 2. XRD patterns of raw materials: (a) Al_4C_3, (b) Si, and (c) mechanically milled powders.

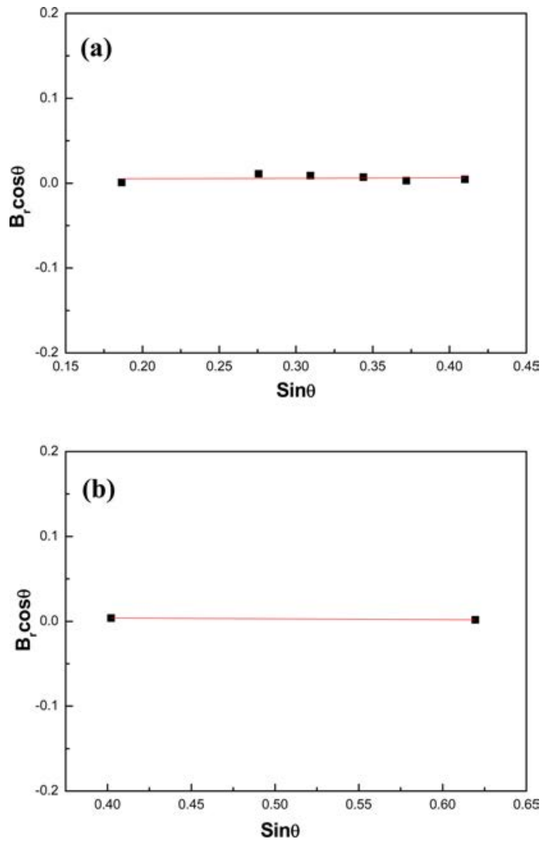

Fig. 3. Plot of $B_r \cos\theta$ versus $\sin\theta$ of (a) Al_4C_3, and (b) Si in the high energy ball milled powders.

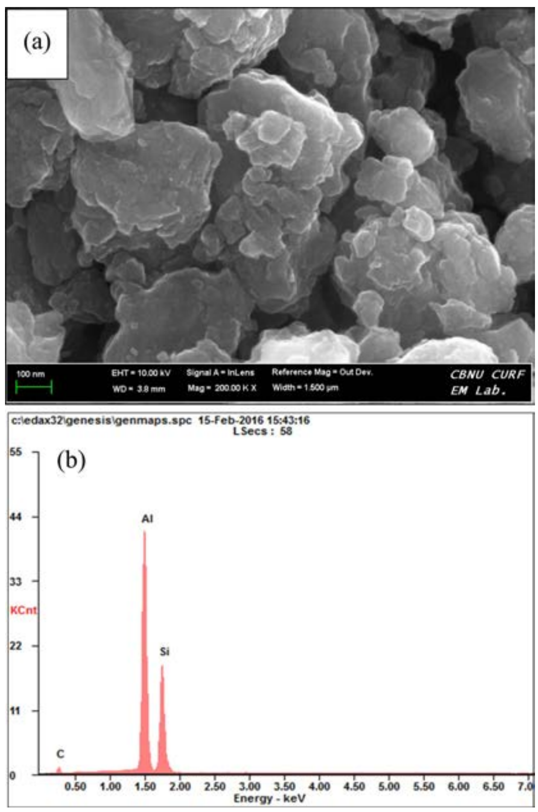

Fig. 4. FE-SEM image (a) and EDS (b) of $Al_4C_3 + 3$ Si powders milled by high energy ball milling for 10 hrs.

composite obtained within short time are as follows. Firstly, the heating rate is very high which can block grain growth during sintering. Secondly, application of pressure during the sintering increases driving force for sintering [14]. The relative density increased with increase in applied pressure during the sintering [15]. Thirdly, the applied current enhanced sintering because Joule heating is created at contact point of the powders, the presence of plasma in pores separating powder particles cleans surface of powders, the wettability and diffusion of atoms is improved under the electric field due to electromigration [16-18].

Vickers hardness measurements were made on polished sections of the 4Al-3SiC composite using a 20 kg_f load and a 15 sec dwell time. The calculated

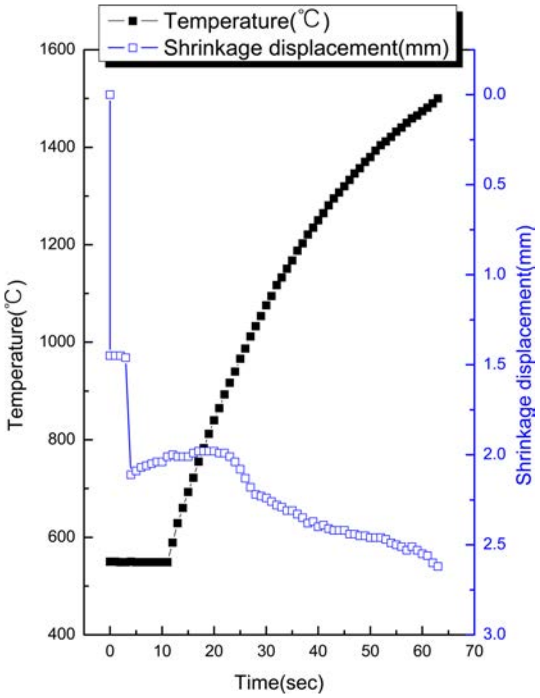

Fig. 5. The variation of temperature and shrinkage displacement with heating time during the synthesis and sintering of Al_4C_3 + 3 Si powders.

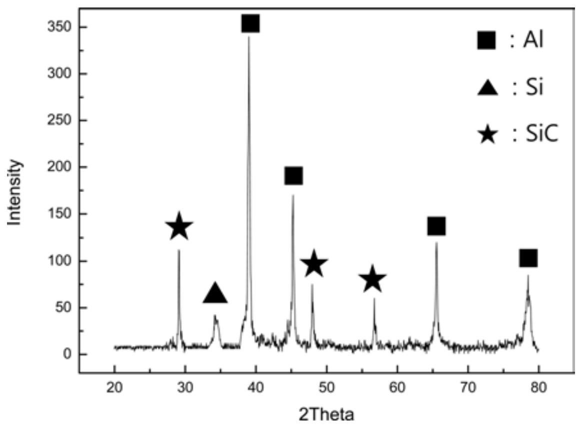

Fig. 6. XRD patterns of 4Al-3SiC composite sintered from high energy ball milled powders.

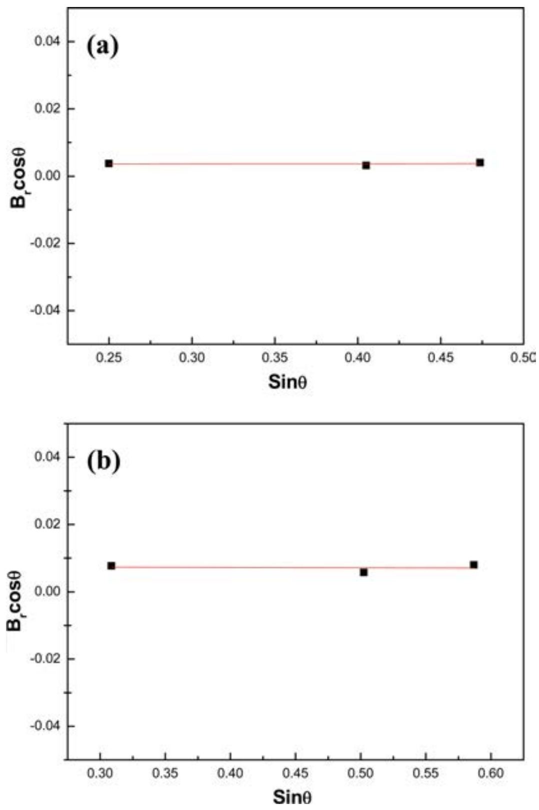

Fig. 7. Plot of Brcosθ versus sinθ of Al (a) and SiC (b) in composite sintered from high energy ball milled powders.

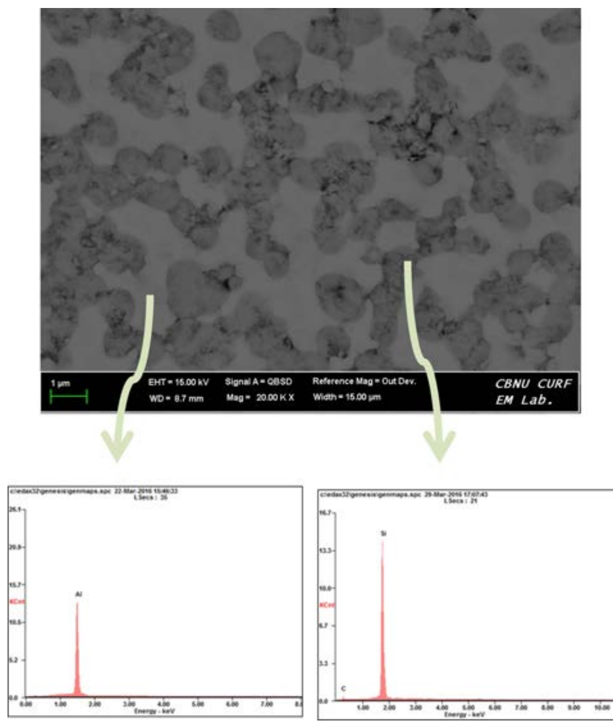

Fig. 8. FE-SEM image and EDS of 4Al-3SiC composite sintered from high energy ball milled powders.

hardness value of 4Al-3SiC composite sintered at 1500 °C from high energy ball milled powders were 651 kg/mm^2. These values represent an average of five measurements. Indentations with large enough loads produced median cracks around the indentation. The length of these cracks permits an estimation of the fracture toughness of the material. From the length of these cracks, fracture toughness values can be determined using the equation by Anstis et al. [19]. As in the case of hardness values, the toughness values were derived from the average of five measurements. The toughness values of composites obtained from high energy ball milled powders are 7 MPa·m$^{1/2}$. A typical indentation pattern for the 4Al-3SiC composite is shown in Fig. 9(a). Typically, one to three additional cracks were observed to propagate from the indentation corner. A higher

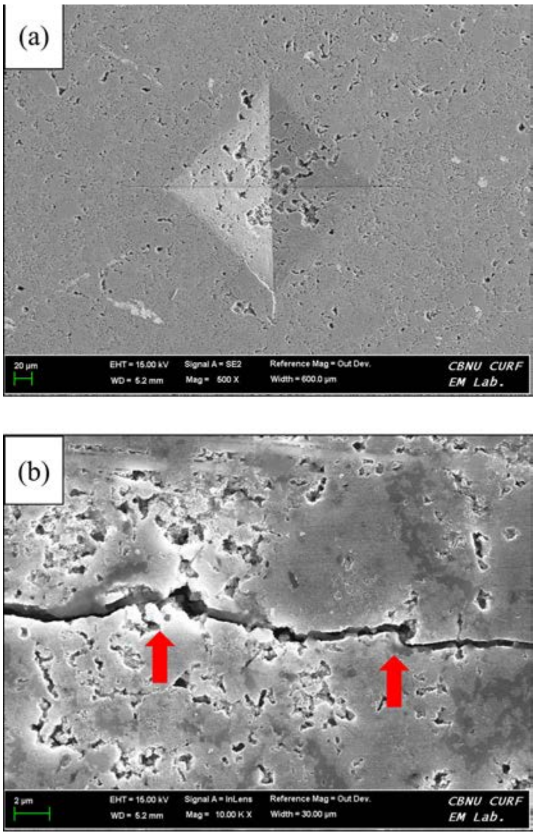

Fig. 9. (a) Vickers hardness indentation and (b) median crack propagating in the 4Al-3SiC composite sintered from high energy ball milled powders.

magnification view of the indentation median crack in the composite is shown in Fig. 9(b). This shows that the crack propagates in a deflective (↑) manner. This is believed to suggest that Al and SiC in the composite may deter the propagation of cracks. The fracture toughness of 4Al-3SiC composite is higher than that of monolithic SiC reported as 2 MPa·m$^{1/2}$ [20].

Conclusions

Nanopowders of Al_4C_3 and Si were fabricated by high energy ball milling. Using the high-frequency induction heated sintering method, the densification of nanostructured 4Al-3SiC composite was accomplished from mechanically activated powders within duration of two minutes. The average grain sizes of Al and SiC prepared by HFIHS were lower than 100 nm. The average hardness and fracture toughness values obtained from mechanically activated powders were 651 kg/mm^2 and 7 MPa·m$^{1/2}$, respectively. The fracture toughness of the 4Al-3SiC composite is higher than that of monolithic SiC because Al and SiC in the composite may deter the propagation of cracks.

Acknowledgments

This research was financially supported by the Ministry of Trade, Industry and Energy (MOTIE) and Korea Industrial Complex Corporation (KICOX) through the Industrial Complex (R & BD) Capacity Enhancement (Project Name: Development of high-strength (350 MPa) composite materials through waste recycling, Project Number: RHN16035) and this research was supported by Basic Science Research Program though the National Research Foundation of Korea (NRF) funded by the Ministry of Education (2015R1D1A1A01056600) and this work was supported by the Korea Institute of Energy Technology Evaluation and Planning (KETEP) and the Ministry of Trade, Industry & Energy(MOTIE) of the Republic of Korea (No. 20164030201070).

References

1. L. Ceschini, G. Minak, A. Morri, Composites Science and Technology 66 (2006) 333-342
2. M. Ohyanagi, T. Yamamoto, H. Kitaura, Y. Kodera, T. Ishii, Z.A. Munir, Scripta Materialia 50 (2004) 111-114.
3. B.W. Kwak, S.J. Lee and I.J. Shon, Korean J. Met. Mater. 54 (2016) 313-321.
4. B.W. Kwak, S.J. Oh, B.S. Kim, J.K. Yoon, and I.J. Shon, Korean J. Met. Mater. 54 (2016) 180-186.
5. S.M. Kwon, N.R. Park, J.W. Shin, S.H. Oh, B.S. Kim, and I.J. Shon, Korean J. Met. Mater. 53 (2015) 555-562.
6. I.J. Shon, H.G. Jo, B.S. Kim, J.K. Yoon, and K.T. Hong, Korean J. Met. Mater. 53 (2015) 474-479.
7. F. Charlot, E. Gaffet, B. Zeghmati, F. Bernard, J. C. Liepce, Mater. Sci. Eng. A262 (1999) 279-278.
8. B.R. Kang, J.K. Yoon, K.T. Hong, and I.J. Shon, Met. Mater. Int. 21[4] (2015) 698-703.
9. M.K. Beyer, H. Clausen-Schaumann, Chem. Rev. 105 (2005) 2921-2948.
10. S.Y. Jeong, B.M. Moon, J.K. Yoon, K.T. Hong and I.J. Shon, Journal of Ceramic Processing Research 16[5] (2015) 472-478.
11. B.R. Kang and I.J. Shon, Korean J. Met. Mater. 53 (2015) 320-325.
12. I.J. Shon, H.S. Kang, J.M. Doh, and J.K. Yoon, Met. Mater. Int. 21[2] (2015) 345-349.
13. C. Suryanarayana, and M.G. Norton, X-ray Diffraction: A Practical Approach, Plenum Press, New York, 1998.
14. R.L. Coble, J. Appl. Phys. 41 (1970) 4798-4807.
15. H.C. Kim, H.K. Park, I.J. Shon, I.Y. Ko, Journal of Ceramic Processing Research **7** (2006) 327-331.
16. Z. Shen, M. Johnsson, Z. Zhao, M. Nygren, J. Am. Ceram. Soc. 85 (2002) 1921-7.
17. Y. Gu, P. Shen, N.N. Yang, K.Z. Cao, Journal of Alloys and Compounds 586 (2014) 80-86.
18. J.E. Garay, U. Anselmi-Tamburini, Z.A. Munir, S.C. Glade, P. Asoka- Kumar, Appl Phys Lett 85 (2004) 573-5.
19. G.R. Anstis, P. Chantikul, B.R. Lawn, D.B. Marshall, J. Am. Ceram. Soc. 64 (1981) 533-538
20. I.J. Shon, H.S. Kang, N.R. Park and I.Y. Ko, Advanced Materials Research 123-125 (2010) 635-638.